Structure of an RNA Internal Loop Consisting of Tandem C-A$^+$ Base Pairs[†,‡]

Se Bok Jang, Li-Wei Hung, Young-In Chi, Elizabeth L. Holbrook, Richard J. Carter, and Stephen R. Holbrook*

Melvin Calvin Building, Structural Biology Department, Physical Biosciences Division, Lawrence Berkeley National Laboratory, University of California, Berkeley, California 94720

Received April 3, 1998; Revised Manuscript Received June 24, 1998

ABSTRACT: The crystal structure of the RNA octamer 5′-CGC(CA)GCG-3′ has been determined from X-ray diffraction data to 2.3 Å resolution. In the crystal, this oligomer forms a self-complementary double helix in the asymmetric unit. Tandem non-Watson−Crick C-A and A-C base pairs comprise an internal loop in the middle of the duplex, which is incorporated with little distortion of the A-form double helix. From the geometry of the C-A base pairs, it is inferred that the adenosine imino group is protonated and donates a hydrogen bond to the carbonyl group of the cytosine. The wobble geometry of the C-A$^+$ base pairs is very similar to that of the common U-G non-Watson−Crick pair.

The picture of RNA molecules being structurally and functionally limited by the use of only four building blocks and by the rules of Watson−Crick base pairing is undergoing a radical change. Noncanonical base pairing within double-helical regions of RNA has been structurally characterized (*1*−*5*) and shown to be functionally important as binding sites for protein (*6*, *7*) and RNA (*8*), in active sites of catalytic RNA (*9*), and in bending RNA into a folded form (*10*, *11*). Several of the noncanonical base pairs are polymorphic (*12*, *13*), assuming a different pairing geometry depending on their environments or the solution conditions. We must also consider that at least some of the bases involved in noncanonical interactions may exist in different charged or protonated forms in different environments. For example, protonation of adenine and cytosine has been observed in the formation of C-A$^+$ (*14*) and C-C$^+$ (*15*, *16*) base pairs.

We report here the 2.3 Å resolution (Table 1) X-ray structure of an RNA octamer which in the crystal forms a double helix incorporating tandem C-A−A-C base pairs bounded by standard Watson−Crick pairs. From the geometry of these noncanonical base pairs, it is inferred that they are C-A$^+$ pairs with a protonated N1 of the adenine donating a hydrogen bond to the cytosine carbonyl group. This "wobble" C-A$^+$ base pairing is structurally similar to, and in some cases may be a substitute for, the more common U-G wobble pair.

Table 1: Refinement Statistics

resolution (Å)	30.0−2.3
number of measurements	25 094
number of unique reflections	2101
number of reflections used in refinement	2030
R_{merge}[a] (%) (in last shell, 2.38−2.30 Å)	4.4 (34.0)
completeness (%) (in last shell, 2.38−2.30 Å)	96.8 (80.2)
I/σ in last shell (2.38−2.30 Å)	4.5
space group	*R*32
cell dimensions	$a = b = 42.737$ Å, $c = 123.9$ Å, $\alpha = \beta = 90.0°$, $\gamma = 120.0°$
number of non-hydrogen RNA atoms (per double helix)	336
number of solvent molecules (per unique strand)	30
R-factor (%) ($F \geq 2.5\sigma$) (1549 reflections between 8 and 2.3 Å)	20.7
R_{free} (146 reflections) (%)	26.3
rms deviations from ideality in bond length (Å)	0.0035
rms deviations from ideality in bond angle (deg)	0.867

[a] $R_{merge} = 100\sum_{hkl}\sum_i|I_i - \langle I\rangle|/\sum_{hkl}\sum_i I_i$, where I_i is the *i*th measurement and $\langle I\rangle$ is the weighted mean of all measurements of *I*.

MATERIALS AND METHODS

Synthesis, Crystallization, and Data Collection. The octaribonucleotide rCGCCAGCG was chemically synthesized (Oligos, Etc.) and purified by anion exchange (DEAE-5PW TSK-Gel, TosoHaas) FPLC[1] with a linear salt gradient from 0.4 to 2.0 M sodium acetate and 50 mM Tris-HCl (pH 6.8−7.3). Crystals were grown at room temperature by the hanging drop vapor diffusion method from a 2.4 μL drop of a solution of 2 mM RNA mixed with an equal volume of the reservoir solution consisting of 20 mM NaCl, 5 mM $MgCl_2$, 2 mM spermine tetrahydrochloride, and 35% MPD (2-methyl-2,4-pentanediol). The crystals were originally grown from a buffer of 50 mM sodium cacodylate (pH 6.5), but superior crystals were later grown from a buffer of 100 mM sodium cacodylate (pH 5.5). The crystals grown at pH 6.5 were thin hexagonal plates with a maximum dimension 100 μm, while those grown at the lower pH were rods that grew to dimensions of 350 μm × 40 μm × 40 μm.

X-ray data were collected on a Rigaku R-axis IIC imaging plate system using CuKα radiation ($\lambda = 1.5418$ Å) and ϕ

[†] This work was supported by NIH Grant, NIGMS, GM 49215 to S.R.H. Financial support was provided to S.B.J. by the Korean Science and Engineering Foundation (KOSEF).

[‡] The refined coordinates of the CA8 duplex have been deposited in the Nucleic Acids Database (ID code AR0001; *39*).

* To whom correspondence should be addressed. Fax: (510) 486-6059. Phone: (510) 486-4304. E-mail: srholbrook@lbl.gov.

[1] Abbreviations: DEAE, diethylaminoethyl; FPLC, fast performance liquid chromatography; MPD, 2,4-methylpentanediol; EPMR, evolutionary protocol for molecular replacement (computer program).

S0006-2960(98)00758-2 CCC: $15.00
Published on Web 08/05/1998

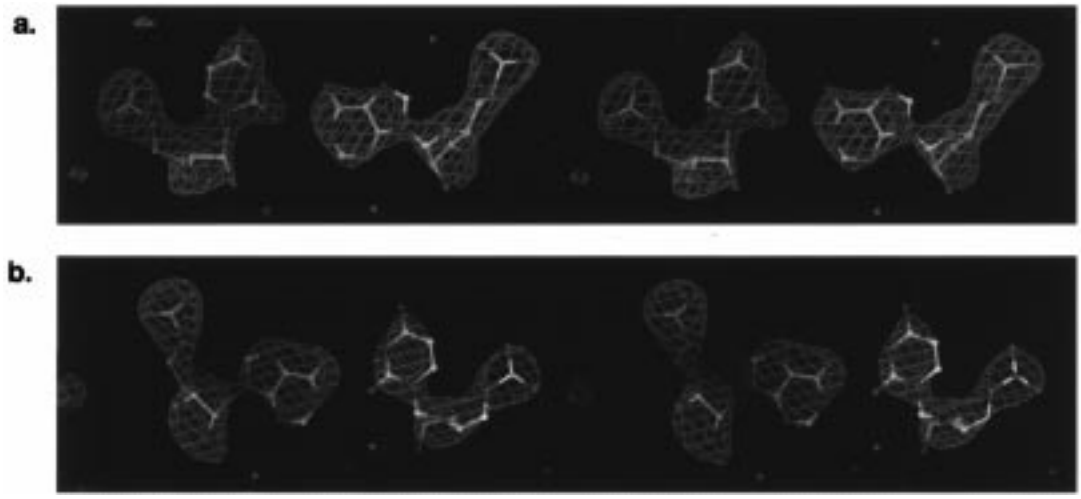

FIGURE 1: Difference electron density calculated after simulated annealing refinement with the C-A$^+$ base-paired oligonucleotides omitted. (a) Stereoview of the C4-A5* pair with the electron density contoured at the 2.5σ level in green superimposed on the nucleotide structure. (b) Stereoview of the A5-C4* pair.

scans with a scan width of 2.0°. Diffraction data were originally collected at room temperature to a resolution of 3.0 Å. When the crystals were flash-frozen in a nitrogen gas stream at 100 K (Oxford cryostream), the resolution was extended anisotropically to a maximum of 2.3 Å in the *h* and *k* directions. Diffraction data were collected on several cryogenically cooled crystals grown under the same conditions. Some of these clearly belonged to space group *C*2 with three unique double helices per asymmetric unit (a = 74.7 Å, b = 43.18 Å, c = 48.72 Å, $\alpha = \gamma = 90°$, and β = 120.62°), while the data collected on other crystals were more compatible with the related space group *R*32 with one double helix per asymmetric unit ($a = b$ = 42.737 Å, c = 123.9 Å, $\alpha = \beta = 90°$, and $\gamma = 120°$). A total of 25 094 reflections were measured which reduced to 2101 unique reflections. Of these, 2030 reflections were used in the structure solution and refinement. This represents 96.8% of a complete 2.3 Å data set. The R_{merge} for the intensity data was 4.4% as shown in Table 1.

Structure Determination. The structure was determined by the molecular replacement method using the EPMR program (C. R. Kissinger and D. K. Gehlhaar, Agouron Pharmaceuticals, Inc.). The search model was constructed from an RNA solution structure (*17*) of $(GCGGACGC)_2$ by substituting the base pairs with the sequence of our construct. The structure was intially solved in the *C*2 cell by locating three independent duplexes. The solution for the first molecule from a six-parameter search using the data between 15.0 and 4.0 Å had a correlation coefficient of 0.510 and was used as a partial structure in the subsequent search for the second molecule. The solutions of two molecules and all three molecules in the asymmetric unit had correlation coefficients of 0.705 and 0.780, respectively. The refined structure from the *C*2 cell was then used as the search model for the *R*32 cell. The correlation coefficient for the EPMR solution was 0.815 with an *R*-factor of 38.3% for data between 15.0 and 3.0 Å resolution, indicating that the structure was the same in both space groups.

Model Refinement. The 2.3 Å resolution data set collected with the flash-frozen crystal was used for further crystallographic refinement (*18*). An overall anisotropic *B*-factor correction was applied to the diffraction data. A total of

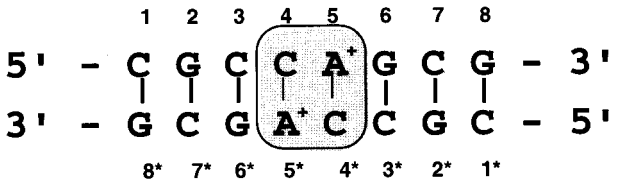

FIGURE 2: Schematic diagram of the CA8 duplex as characterized in crystals of the octamer ribonucleotide r(CGCCAGCG) with the numbering scheme used in the text indicated. The three terminal base pairs on each end are standard Watson−Crick pairs, while the two middle base pairs form an internal loop of tandem noncanonical C-A$^+$ pairs as indicated by the shaded boxing.

10% of the data was randomly selected for cross-validation of the refinement process using the R_{free} (*19*). Initial positional refinement of the rigid-body-refined model using 10.0−3.0 Å data followed by group *B*-factor refinement dropped the R_{free} to 33.4%. The refinement was then continued using simulated annealing protocols against a maximum likelihood target (*20*) and a correction for the bulk solvent continuum. Restraints were placed on bond lengths, bond angles, nonbonded contacts, temperature factors of neighboring atoms, the planarity of the base pairs, and the sugar pucker of the nucleotides in the Watson−Crick pairs using the parameter set developed by Berman and co-workers (*21*). $F_o - F_c$ difference Fourier maps were calculated at regular intervals to monitor the refinement and locate bound water sites. Solvent molecules (all regarded as water) were added conservatively with due regard for their environment, including potential interactions with hydrogen bond partners. At the end of the refinement, the standard crystallographic *R*-factor for data between 8.0 and 3.0 Å, excluding those with an F_{obs} of less than $2.5\sigma F_{obs}$, was 20.7% and R_{free} was 26.3%. Electron density was clearly defined for all nonhydrogen atoms. The final difference electron density for the noncanonical C-A base pairs is shown in Figure 1.

RESULTS AND DISCUSSION

Structure of the Double Helix. In the crystal, two strands of the RNA octamer, rCGCCAGCG, form an A-type double helix (CA8 duplex) incorporating an internal loop consisting of tandem C-A base pairs as shown schematically in Figure 2. These duplexes stack head to head to produce pseudo-

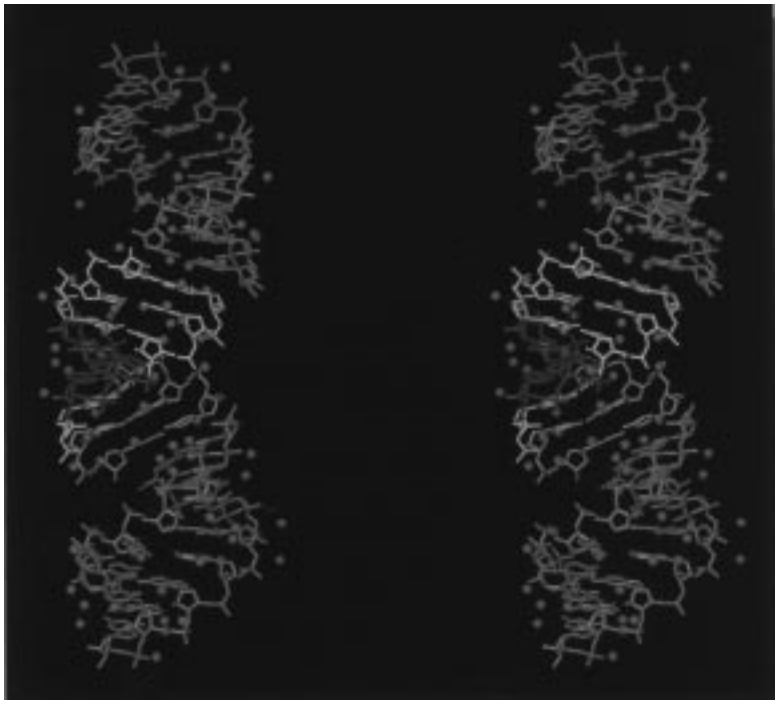

FIGURE 3: Stereoview of the CA8 duplex in yellow with the internal loop (C-A$^+$ pairs) in green. Duplexes related by crystallographic symmetry stack head to head (tail to tail) above and below to form pseudoinfinite helices throughout the crystal. Blue spheres along the helices represent bound water molecules.

Table 2: Torsion Angles

	α (P−O5′)	β (O5′−C5′)	γ (C5′−C4′)	δ (C4′−C3′)	ε (C3′−O3′)	ζ (O3′−P)	χ (C1′−N)
Cyt 1	−	−	−	84	−149	−76	−166
Cyt 1*	−	−	−	77	−154	−74	−161
Gua 2	−69	174	51	91	−139	−76	−168
Gua 2*	−54	168	52	81	−143	−78	−165
Cyt 3	−59	169	53	78	−140	−71	−161
Cyt 3*	−65	173	51	81	−143	−68	−153
Cyt 4	−56	165	49	82	−162	−95	−156
Cyt 4*	−61	−178	39	79	−174	−82	−152
Ade 5	−58	−178	45	80	−142	−67	−165
Ade 5*	**155**	−170	**177**	85	−130	−72	178
Gua 6	−58	171	49	79	−157	−74	−165
Gua 6*	−63	175	54	81	−153	−72	−167
Cyt 7	−65	171	56	83	−149	−79	−167
Cyt 7*	−65	174	55	82	−157	−69	−164
Gua 8	−60	168	58	75	−	−	−158
Gua 8*	−69	−177	55	79	−	−	−151
RNA-A	−62	−180	47	83	−152	−74	−166

infinite helices throughout the crystal as shown in the stereoview of Figure 3. The double helix formed by the octamers is very similar to a standard A-RNA helix. The overall root-mean-square difference between A-RNA and the CA8 duplex is only 1.0 Å. When canonical A-form helices are superimposed on the two Watson−Crick ends of the CA8 duplex, the angle between their helix axes is 5.2° and their displacement only 0.7 Å, indicating that the ends of the CA8 duplex form collinear helices with little global perturbation introduced by the presence of the tandem C-A base pairs.

A regular, linear helix fit to the CA8 duplex has an average helical rotation of 32.2° with a displacement of 2.4 Å (compared to 32.7° and 2.8 Å, respectively, for A-RNA). Alternatively, a nonlinear helix calculated by the CURVES (*22*) program through these eight base pairs bends by 21°, resulting in an offset from a linear axis of 1.3 Å for the C-A base pairs. The average twist and rise for this curved helix are 32.3° and 2.9 Å, respectively. The CURVES calculation of helical bending has been previously shown to differ from end-to-end interhelical angles when it is applied to oligomers containing runs of noncanonical base pairs (*23*). The groove widths are not well-defined for this short helical fragment, although it does appear that the minor groove is slightly compressed (width of 9.1−10.3 Å) with respect to canonical A-RNA (11.1 Å). The helical diameter varies from 19.4 to 20.1 Å compared with 17.4 Å for a standard A-form helix.

The torsion angles of the two nonidentical strands of the CA8 duplex are given in Table 2 and compared with A-RNA. The major deviations from A-form dihedral angles are the α (P−O5′) and γ (C5′−C4′) angles between the C-A mispairs on the second strand which change from gauche-(−), gauche(+) to trans, trans.

The helical twist angles and other base pair step parameters are shown in Table 3 and compared with those of a canonical A-form helix. Although large local variations are observed in rise, twist, and roll, the average parameters describing the

Table 3: Base Pair Step Parameters[a]

base pair step	rise (Δz) (Å)	twist (deg)	tilt (deg)	roll (deg)	shift (Δx) (Å)	slide (Δy) (Å)
C1-G8*−G2-C7*	3.08	36.4	−7.8	0.9	0.1	0.3
G2-C7*−C3-G6*	2.98	30.2	−0.9	−3.0	0.4	−0.4
C3-G6*−C4-A5*	2.89	47.7	−0.4	−0.2	1.7	0.0
C4-A5*−A5-C4*	2.59	0.3	−4.5	20.0	−1.2	−3.0
A5-C4*−G6-C3*	3.12	43.6	6.1	8.7	−0.8	0.3
G6-C3*−C7-G2*	2.82	34.6	−0.1	−2.3	−0.2	0.2
C7-G2*−G8-C1*	3.08	33.3	10.4	−1.5	−0.7	−0.1
average	2.94	32.3	0.4	3.2	−0.1	−0.4
RNA-A	2.81	32.7	0.0	0.0	0.0	0.0

[a] Calculated by the CURVES program.

Table 4: Intermolecular Contacts

Direct Interhelical Hydrogen Bonds

residue 1	atom 1	atom 2	residue 2	distance (Å)
A5	O2′	N2	G6	3.07
G6	O1P	O2′	C7	2.45
A5*	O1P	O2′	G6*	2.71
A5*	O2′	O2′	A5*	3.34
G6*	O2′	O2′	G6*	3.01

Water-Mediated Interhelical Hydrogen Bonding

residue 1	atom 1	bridging water 2	residue 3	atom 3	1−2 distance (Å)	2−3 distance (Å)
C7	O2′, O3′	Wat 1	C7	O2P	3.4, 3.3	2.9
C4*	O2′	Wat 25	A5*	N3	3.4	2.5
A5*	O4′	Wat 25	A5*	N3	3.1	2.5
G6*	O2P	Wat 22	G6*	O2′, O3′	3.3	2.9, 3.1
A5	O2′	Wat 30	C4*	O2′	2.6	2.8
G6	O1P	Wat 2	C7	O2	2.7	3.1
G6	O1P	Wat 9	G8	O4′	3.0	3.0
C1	O5′	Wat 4	G8*	N7	2.9	3.4
G8*	O3′	Wat 5	C7*	O2′	3.3	2.7

base pair steps are very similar to those of a canonical RNA-A helix. This also indicates that the tandem C-A mismatches can be incorporated into a double helix with little distortion in either overall helical twist (turn) or length.

The 30 bound water molecules identified in the crystal structure are also shown in Figure 3. Of 61 water−RNA interactions, 27 are with base atoms (seven with guanosine O6 and six with cytosine N4) and 34 with backbone atoms (13 with phosphate oxygens and nine with ribose O2′).

In addition to the formation of pseudoinfinite helices through stacking, as shown in Figure 3, the helices interact through direct hydrogen bonding and through hydrogen bonds with bridging water molecules as shown in Table 4. All direct hydrogen bonds involve at least one backbone O2′, and half of them are O2′−O2′ interactions (Table 4). Water-mediated intermolecular hydrogen bonding primarily involves ribose O2′ moieties on one helix, although base atoms are also involved in this case.

The restrained atomic thermal or mobility parameters (*B*-factors) do not show large or systematic variation. The mobility of the C-A pairs is no greater than that of the Watson−Crick base pairs, as previously observed for the nonstandard base pairs of other internal loops (*1*, *2*). The region of greatest mobility is the C1*-G2* phosphodiester backbone.

Noncanonical C-A Base Pairing. The C-A base pairing geometry is illustrated in Figure 4. In the crystal, the two

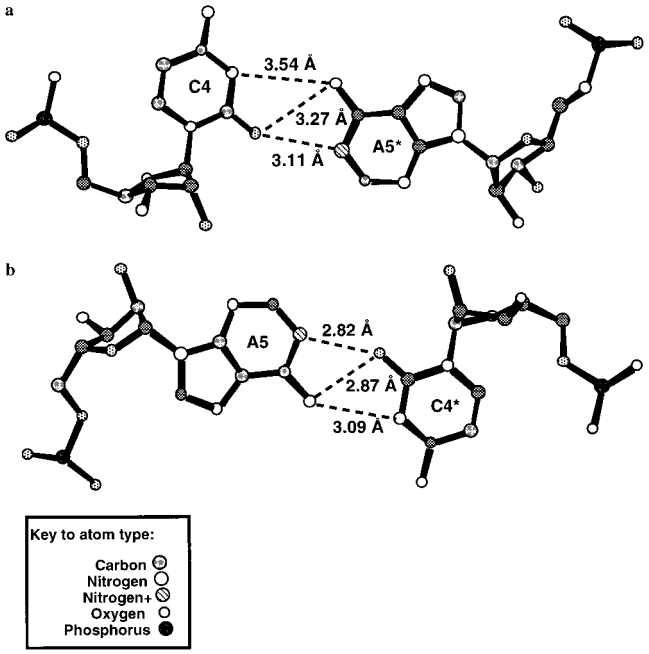

FIGURE 4: Noncanonical C-A$^+$ base pairs observed in the CA8 crystal structure. The two C-A$^+$ pairs (a and b) are not crystallographically symmetric and show significant differences in base pairing geometry. (a) The C4-A5* base pair with hydrogen bonding distances in angstroms shown by dashed lines. (b) The A5-C4* base pair with hydrogen bonding indicated. Bifurcated hydrogen bonding is observed in both cases. Atom types are denoted by shading as indicated in the key.

C-A base pairs are not symmetrically related and exhibit somewhat different hydrogen bonding patterns as illustrated in Figure 4. Stereochemical analysis suggests that the adenosine is protonated at the N1 position, forming N1H-(A)$^+$···O2(C) and N6H(A)···N3(C) hydrogen bonds. This type of base pairing has been previously observed in the crystal structure of a DNA oligomer (*14*) and the NMR structure of an RNA hairpin loop (*24*).

The tandem C-A$^+$−A$^+$-C pairs have a near 0° helical twist angle between them (Table 3). This unwinding is balanced by an overwinding of 10−15° at the junction with the surrounding Watson−Crick pairs. Large roll angles around the C-A pairs (Table 3) are responsible for the overall helical bending described above. A characteristic feature of this structure is the cross-strand purine stacking between the protonated adenosines of the tandem C-A pairs. The stacking between the C-A pairs and the stacking of the C-A pairs on the bounding Watson−Crick pairs are shown in Figure 5.

Stability of C-A$^+$ Base Pairs. Thermodynamic measurements have been taken on a series of RNA oligomers incorporating tandem noncanonical mispairs (*25*). Tandem C-A$^+$ pairs were shown to be less stable than tandem G-U, G-A, and U-U pairs, but at least as stable as U-C, C-C, and A-A pairs (*26*). Thermodynamic studies show a small pH dependence of the melting temperature for tandem C-A and A-C pairs; the melting temperature increases 3−5 °C on lowering the pH from 7.0 to 5.5. The pH dependence of C-A$^+$ base pair stability in DNA has also been studied by UV melting experiments (*27*). The maximum stability of a C-A$^+$ base pair in a DNA oligomer occurred near pH 5.3, but was shown to be highly dependent on the flanking bases, presumably due to dipole and stacking interactions. Consistent with the pH dependence of formation of C-A$^+$ base

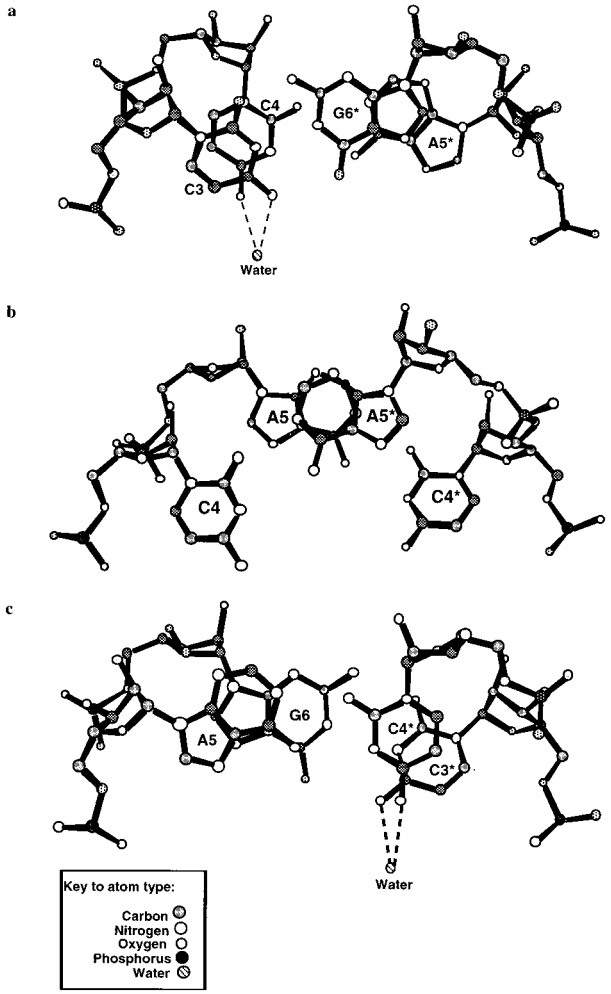

FIGURE 5: Base stacking between C-A$^+$ pairs and their bounding C-G Watson−Crick pairs. In addition to stacking interactions, helical twist angles (Table 3) are also apparent. (a) C3-G6* Watson−Crick base pair stacking on a C4-A5* noncanonical pair. (b) Stacking between the tandem C4-A5*−A5-C4* bases forming C-A$^+$ pairs. Note the cytosines are completely unstacked on the 3′ side. (c) Stacking between the A5-C4* mispair and the standard G6-C3* pair. In panels a and c, a tightly bound water molecule is shown which bridges the N4 atoms of the stacked cytosines as shown by the dashed lines.

pairs is the dramatic increase we observed in crystal size and quality on lowering the pH of crystallization from 6.5 to 5.5 (see Materials and Methods).

No integral water molecules are involved in stabilizing the C-A base pairs as seen for some other non-Watson−Crick pairs (*1*). However, bound water molecules bridge the cytosines (N4) of the C-A$^+$ mispairs and the neighboring C-G Watson−Crick pairs as shown in Figure 5. The *B*-factors of these bridging water molecules are similar to those of the cytosines themselves, indicating that they are tightly bound. Consistent with this finding, thermodynamic analysis of this duplex sequence (C-G−C-A$^+$) indicates greater enthalpic stabilization and entropic cost compared to those of a related octamer duplex in which the C-A pairs are bounded by G-C pairs (*25*, *26*).

Wobble Base Pairing. Of the noncanonical base pairs, the so-called wobble pair U-G (or T-G) is the most stable and also the most common in both RNA and DNA. Two characteristics of U-G base pairing are (1) formation of two base pair hydrogen bonds, one of which is between the purine imino hydrogen and the pyrimidine carbonyl oxygen; and

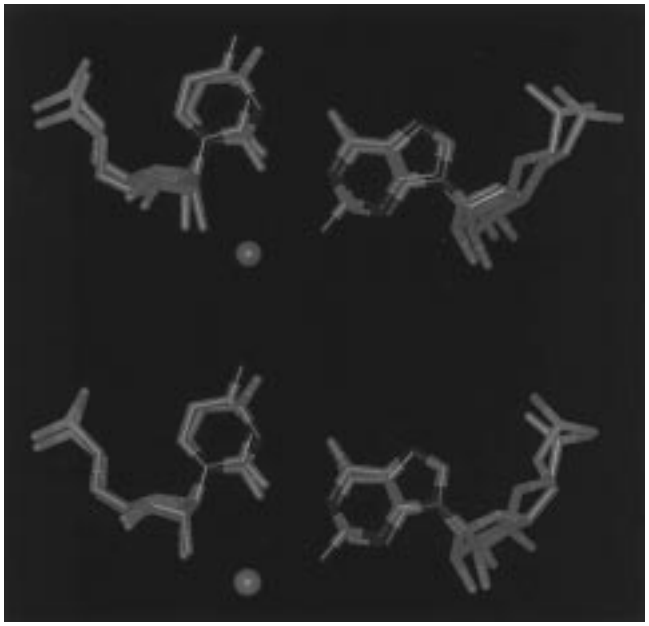

FIGURE 6: Comparison of C-A$^+$ and U-G wobble base pairs. The C-A$^+$ pairs are from the CA8 duplex, and the U-G pair is from the crystal structure of r(CGACUUCGGUCC)$_2$ (*1*). The C-A$^+$ wobble pair was superimposed on the U-G pair by least-squares fitting. The upper view shows C4-A5* superimposed on a U-G pair The lower view shows A5-C4* compared to U-G. An integral water molecule linking the guanine amino group to the uracil O2′ is shown as a red sphere. Atom types are color coded as follows: carbon, green; nitrogen, blue; oxygen, red; and phosphorus, magenta.

(2) translation of the pyrimidine toward the major groove and purine toward the minor groove. These characteristics are shared with the structurally isomorphous C-A$^+$ base pair which has a similar C1′−C1′ distance and λ glycosyl angle (*14*). Consistent with this structural similarity, C-A$^+$ base pairs have been found to substitute for U-G pairs in certain sites of biological RNAs (*28*−*30*). Figure 6 compares the geometry of a typical U-G pair with that of the C-A$^+$ pairs characterized in this structure. One difference between U-G and C-A$^+$ pairs, as shown in Figure 6, is the integral water molecule found to bridge the guanine amino group and the 2′-hydroxyl of the sugar on its uridine partner.

Occurrence of C-A$^+$ Base Pairs in Biological Systems. The formation of C-A$^+$ base pairs has been verified in several RNA motifs, including ribozyme cleavage sites, protein recognition sites, and ribosomal RNA motifs. In other cases, C-A$^+$ base pairs can substitute for U-G wobble pairs. The identification and characterization of C-A$^+$ wobble pairing in these systems will undoubtedly lead to the discovery of other examples in biological systems.

Several ribozyme cleavage sites are associated with C-A$^+$ wobble pair formation. The solution structures of the leadzyme (*31*, *32*) and loop A of a hairpin ribozyme (*9*) have been analyzed by NMR methods. The cleavage sites of both ribozymes are found in internal loops immediately following the cytosine of a C-A$^+$ base pair. The wobble base pairing structure of the C-A$^+$ pairs is the same as that observed in our structure. The pK_as for protonation of the adenine in the C-A$^+$ pairs were determined to be 6.2 (hairpin) and 6.5 (leadzyme). The cleavage site of group I introns is characterized by a U-G wobble pair within the P1 helix. Of allpossible base pairings, only a C-A$^+$ wobble base pair can substitute for the U-G pair (*33*).

The G3-U70 wobble pair in the acceptor stem of *Escherichia coli* tRNA^{Ala} has been shown to be necessary and sufficient for recognition by its cognate synthetase (*34*, *35*). It has been shown that this G-U mispair can be substituted in vivo by other non-Watson−Crick base pairs, including C-A (and G-A), implying that distortion in the helix induced by mispairing rather than a particular sequence may be responsible for recognition (*30*). The solution structure of the acceptor stem of this tRNA has been determined by NMR and demonstrates how a unique recognition site is provided by the wobble base pairing (*36*).

The 790 loop of 16S ribosomal RNA is a conserved hairpin required for ribosome function (*37*). It is exposed to solvent and located at the interface between the large and small subunits of 70S ribosomes. Mutation of all loop nucleotides indicates that a C-A pair at the base of the loop is required for optimal function and that 50 of 78 selected mutants have the potential to form either the wobble pair A$^+$-C or G-U. Melting studies at pH 5.3 and 7.0 show that the hairpin is more stable by 1.6 kcal/mol (7 °C) at the lower pH, suggesting protonation of the adenosine in the base pair. NMR analysis shows that loops with the A$^+$-C pair replaced by G-U have very similar structures consistent with the functional analysis.

The formation of A$^+$-C wobble pairs presents the opportunity for a conformational switch based on modification of the adenosine protonation by environmental factors such as protein, RNA, or metal binding. It would be surprising if nature did not take advantage of this opportunity. For example, a synthetic DNA oligomer corresponding to a region of the K-ras gene containing an A$^+$-C base pair at a hot spot for mutation was shown to undergo a structural change to a classic wobble conformation as the pH was lowered (*38*).

ACKNOWLEDGMENT

Facilities and equipment were provided through support of the Office of Energy Research, Office of Health and Environmental Research, Health Effects Research Division of the U.S. Department of Energy. Special recognition is due to John SantaLucia and Doug Turner who supplied the initial RNA sample and suggested this project, Katrien Baeyens who first grew the high-pH crystals of this oligomer, and Hendrik DeBondt who collected and reduced the first data set with those crystals.

NOTE ADDED IN PROOF

The crystal structure of a 16-mer RNA duplex incorporating A$^+$-C base pairs of the same conformation as described in this paper was recently determined by B. Pan, S. N. Mitra, and M. Sundaralingam (private communication).

REFERENCES

1. Holbrook, S. R., Cheong, C., Tinoco, I., Jr., and Kim, S.-H. (1991) *Nature 353*, 579−581.
2. Baeyens, K. J., DeBondt, H. L., and Holbrook, S. R. (1995) *Nat. Struct. Biol. 2*, 56−62.
3. Baeyens, K. J., De Bondt, H. L., Pardi, A., and Holbrook, S. R. (1996) *Proc. Natl. Acad. Sci. U.S.A. 93*, 12851−12855.
4. Carter, R. J., Baeyens, K. J., SantaLucia, J., Turner, D. H., and Holbrook, S. R. (1997) *Nucleic Acids Res. 25*, 4117−4122.
5. Lietzke, S. E., Barnes, C. L., Berglund, J. A., and Kundrot, C. E. (1996) *Structure 4*, 917−930.
6. Bartel, D. P., Zapp, M. L., Green, M. R., and Szostak, J. W. (1991) *Cell 67*, 529−536.
7. Dallas, A., and Moore, P. B. (1997) *Structure 5*, 1639−1653.
8. Cate, J. H., Gooding, A. R., Podell, E., Zhou, K., Golden, B. L., Szewczak, A. A., Kundrot, C. E., Cech, T. L., and Doudna, J. A. (1996) *Science 273*, 1696−1699.
9. Cai, Z., and Tinoco, I., Jr. (1996) *Biochemistry 35*, 6026−6036.
10. Cate, J. H., Gooding, A. R., Podell, E., Zhou, K., Golden, B. L., Kundrot, C. E., Cech, T. R., and Doudna, J. A. (1996) *Science 273*, 1678−1685.
11. Battiste, J. L., Tan, R., Frankel, A. D., and Williamson, J. R. (1994) *Biochemistry 33*, 2741−2747.
12. SantaLucia, J., Jr., Kierzek, R., and Turner, D. H. (1990) *Biochemistry 29*, 8813−8819.
13. Heus, H. A., Wijmenga, S. S., Hoppe, H., and Hilbers, C. W. (1997) *J. Mol. Biol. 271*, 147−158.
14. Hunter, W. N., Brown, T., Anand, N. N., and Kennard, O. (1986) *Nature 320*, 552−555.
15. Boulard, Y., Cognet, J. A., and Fazakerley, G. V. (1997) *J. Mol. Biol. 268*, 331−347.
16. Yu, A., Barron, M. D., Romero, R. M., Christy, M., Gold, B., Dai, J., Gray, D. M., Haworth, I. S., and Mitas, M. (1997) *Biochemistry 36*, 3687−3699.
17. Wu, M., and Turner, D. H. (1996) *Biochemistry 35*, 9677−9689.
18. Brunger, A. T., Adams, P. D., and Rice, L. M. (1997) *Structure 15*, 325−336.
19. Brunger, A. T. (1992) *Nature 355*, 472−475.
20. Adams, P. D., Pannu, N. S., Read, R. J., and Brunger, A. T. (1997) *Proc. Natl. Acad. Sci. U.S.A. 94*, 5018−5023.
21. Parkinson, G., Vojtechovsky, J., Clowney, L., Brunger, A. T., and Berman, H. M. (1996) *Acta Crystallogr. D52*, 57−64.
22. Lavery, R., and Sklenar, H. (1989) *J. Biomol. Struct. Dyn. 6*, 655−667.
23. Holbrook, S. R. (1997) in *Molecular Modeling of Nucleic Acids* (Neocles, J., Leontis, B., and SantaLucia, J., Eds.) pp 56−76, American Chemical Society, Washington, DC.
24. Puglisi, J. D., Wyatt, J. R., and Tinoco, I., Jr. (1990) *Biochemistry 29*, 4215−4226.
25. SantaLucia, J., Jr., Kierzek, R., and Turner, D. H. (1991) *Biochemistry 30*, 8243−8250.
26. Wu, M., McDowell, J. A., and Turner, D. H. (1995) *Biochemistry 34*, 3204−3211.
27. Brown, T., Leonard, G. A., Booth, E. D., and Kneale, G. (1990) *J. Mol. Biol. 212*, 437−440.
28. Gutell, R. R. (1995) in *Ribosomal RNA: Structure, evolution, processing, and function protein biosynthesis* (Zimmerman, R. A., and Dahlberg, A. E., Eds.) pp 109−126, CRC Press, Boca Raton, FL.
29. Gautheret, D., Konings, D., and Gutell, R. R. (1995) *RNA 1*, 807−814.
30. Gabriel, K., Schneider, J., and McClain, W. H. (1996) *Science 271*, 195−197.
31. Legualt, P., and Pardi, A. (1994) *J. Am. Chem. Soc. 116*, 8390−8391.
32. Legault, P., and Pardi, A. (1997) *J. Am. Chem. Soc. 119*, 6621−6628.
33. Doudna, J. A., Cormack, B. P., and Szostak, J. W. (1989) *Proc. Natl. Acad. Sci. U.S.A. 86*, 7402−7406.
34. Hou, Y.-M., and Schimmel, P. (1988) *Nature 333*, 140−145.
35. McClain, W. H., Chen, Y.-M., Foss, K., and Schneider, J. (1988) *Science 242*, 1681−1684.
36. Ramos, A., and Varani, G. (1997) *Nucleic Acids Res. 25*, 2083−2090.
37. Lee, K., Varma, S., SantaLucia, J. J., and Cunningham, P. R. (1997) *J. Mol. Biol. 269*, 732−743.
38. Boulard, Y., Cognet, J. A., Gabarro-Arpa, J., Le Bret, M., Carbonnaux, C., and Fazakerley, G. V. (1995) *J. Mol. Biol. 246*, 194−208.
39. Berman, H. M., Olson, W. K., Beveridge, D. L., Westbrook, J., Gelbin, A., Demeny, T., Hsieh, S.-H., Srinivasan, A. R., and Schneider, B. (1992) *Biophys. J. 63*, 751−759.

BI980758J